CHIN. PHYS. LETT. Vol. 26, No. 12 (2009) 125204

Proton Acceleration with Nano-Scale Micro-Structured Target by Circularly Polarized Laser Pulse *

JIN Zhang-Ying(金张英)**, SHEN Bai-Fei(沈百飞), ZHANG Xiao-Mei(张晓梅), WANG Feng-Chao(王凤超), WEN Meng(温猛), JI Liang-Liang(吉亮亮), XU Jian-Cai(徐建彩), WANG Wen-Peng(王文鹏)

State Key Laboratory of High Field Laser Physics, Shanghai Institute of Optics and Fine Mechanics, Chinese Academy of Sciences, Shanghai 201800

(Received 8 July 2009)

Two dimensional particle-in-cell simulations are taken to study the interaction of a circularly polarized laser pulse with a nano-scale micro-structured target. The protons which are doped in the rear side of the target experience the electrostatic fields caused by both the radiation pressure driven shock and the target normal sheath at the rear side of the target. A quasimonoenergetic proton bunch with central energy of about 11 MeV and energy spread of $\Delta\varepsilon/\varepsilon$ about 0.18 is achieved by using a 3.45×10^{19} W/cm^2, 66 fs laser pulse. A comparison with the case of linearly polarized laser pulse and the same target condition is considered.

PACS: 52.38.Kd, 52.50.Jm, 52.65.Rr

Energetic ion bunches of short duration and low energy divergence have many potential applications, such as proton radiography, diagnostics for laser-plasma interaction, nuclear physics, fast ignition, etc.[1−5] Many experiments have been performed to achieve such ion bunches based on the mechanism of target normal sheath acceleration (TNSA).[6−9] Theoretical studies have also explored different acceleration mechanisms, such as shock acceleration,[10−13] skin-layer ponderomotive acceleration,[14] laser-breakout afterburner[15] and light pressure acceleration.[16,17] For TNSA, Robinson *et al.*[18] and other groups[7,8] studied the interaction of a linearly polarized (LP) pulse with micro-structured targets. It was found that a heavily proton-doped target fails to generate a good quasimonoenergetic proton beam. Humières *et al.*[19] studied the proton acceleration by combining the shock acceleration and TNSA using LP pulses. They found that the protons initially located in the center of the target, which were first accelerated by a shock and then by the TNSA, were the most energetic. He *et al.*[20] studied ion cascade acceleration from the interaction of a circularly polarized (CP) laser pulse with a 1 μm thickness target without any structure. The ions from the front surface were accelerated by two steps to high energies, however the accelerated protons were not monoenergetic in their simulations. The influence of the laser polarization in the ion acceleration process has also been studied by many groups and the CP laser was proved very promising for producing energetic ions.[11,13,21,22] Yin *et al.*[11] considered the radiation pressure driven shock acceleration dominated over the TNSA and the most energetic ions were accelerated by the shock acceleration not the TNSA. Ji *et al.*[13] did not take the influence of TNSA into consideration because the influence of TNSA could be neglected for their simulation parameters.

In this Letter, we propose a new method using a nano-scale micro-structured target and a CP pulse so that the protons which are doped in the rear side of the target can be accelerated by the combination of shock acceleration and TNSA, and a high-energy, quasimonoenergetic proton bunch can be achieved. Both shock acceleration and TNSA play important roles in the proton acceleration. For the nano-scale target and CP pulse case, the shock quickly transmits to the rear side of the target and the electrostatic field caused by the shock accelerates the protons more efficiently than the LP case. The proton layer experiences both electrostatic fields caused by the radiation pressure driven electrostatic shock and the TNS, and the more energetic protons are produced in the CP case. It should be mentioned that using a CP pulse with a finite spot size, the 'hole-boring' effect will cause that the pulse irradiates the target at oblique incidence and hot electrons can be generated by the electric field component perpendicular to the plasma surface. In addition, the electron heating caused by tightly focused CP pulses has been studied.[23,24] Thus, the TNSA is still possible in the case of CP.

Two-dimensional simulations are made with the particle-in-cell (PIC) code. A circularly polarized laser pulse of wavelength $\lambda_L = 1\,\mu$m enters from the left of the simulation box. The peak intensity of the pulse is $I_L = 3.45\times10^{19}$ W/cm^2, corresponding to the dimensionless amplitude $a_L = eE_L/m_e\omega c = 5/\sqrt{2} \approx 3.5$. The pulse length is $20\lambda_L$ and the focal spot radius is $6\lambda_L$ (full width at half maximum (FWHM)). The simulation box is $100\lambda_L \times 50\lambda_L$ and there are 20000×500 grid cells in the x and y directions, where x is the laser propagation direction. There are 40 particles in each cell. Sixteen CPUs are used to operate the simulations. The target is of width $40\lambda_L$ and

*Supported by the National Key Basic Research Program of China under Grant No 2006CB806004, the National Natural Science Foundation of China under Grant Nos 10675155 and 10834008, Scientific Research Foundation for Awarder of Excellent Doctor Thesis, and President Award of Chinese Academy of Sciences (No 0801051-X00).

**Email: j3i4n52@163.com

© 2009 Chinese Physical Society and IOP Publishing Ltd

thickness $0.32\lambda_L$, located from $x = 40\lambda_L$ to $40.32\lambda_L$, as illustrated in Fig. 1. The front (left) part is composed of heavy (C^{6+}) ions and electrons whose electron density is $n_e = 4.1n_{cr}$, where the critical density $n_{cr} = m\omega_L^2/(4\pi e^2)$. The small part setting in the rear side of the target occupies a region of $40.3 \sim 40.32\lambda_L$ (20 nm) in longitudinal and $-2.5 \sim 2.5\lambda_L$ in transverse and is composed of heavy (C^{6+}) ions (density $n_c = 2.1/6n_{cr}$), protons (density $n_p = 2n_{cr}$) and electrons (density $n_e = 4.1n_{cr}$). The whole target is of charge neutrality.

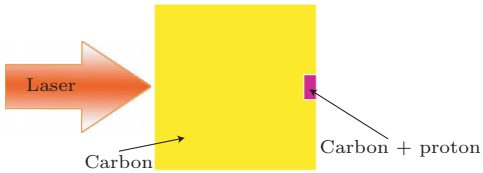


Fig. 1. (Color online) The diagrammatic sketch of the nano-scale micro-structured target.[18]

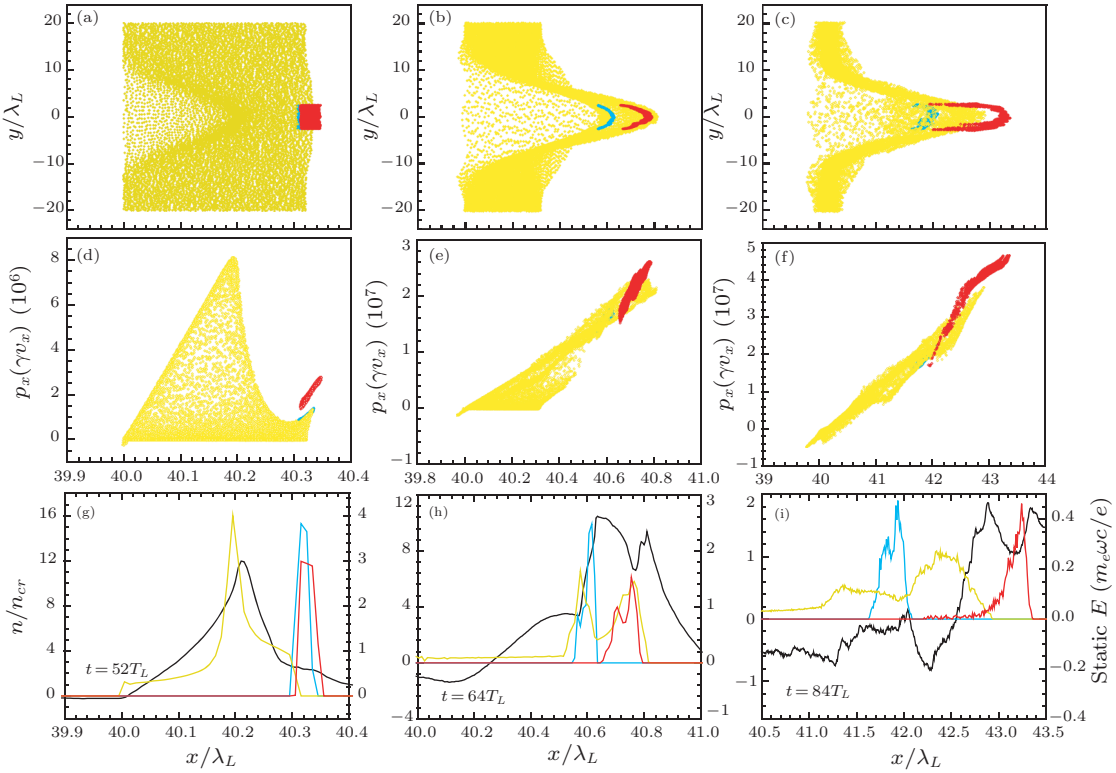


Fig. 2. (Color online) Ion position (top), ion phase space $p_x - x$ (middle) and electrostatic fields with particle densities distribution (bottom) along the x axis plots at different times. The first column for (a), (d) and (g) is at $t = 52T_L$. The second column for (b), (e) and (h) is at $t = 64T_L$. The third column for (c), (f) and (i) is at $t = 84T_L$. The red, cyan and yellow parts in the plots at the top and middle rows (corresponding to Figs. 2(a)–2(f)) represent respectively the protons, the C^{6+} ions which are initially inside the small microdot at the rear side of the target and the other carbon ions. In the Figs. 2(g)–2(i), the black line represents the electrostatic fields, and the cyan, yellow and red lines represent the densities of the C^{6+} ions initially inside the small micro-structure, C^{6+} ions in the other part of target and protons. The charger number densities of the C^{6+} ions (Zn_c) and the protons (n_p) initially located in the microdot at the rear side of the target have been multiplied by 10 to make them easy to be distinguished. Only the particles located in $-2.5\lambda_L < y < 2.5\lambda_L$ are accounted.

The plots of ion position (top), ion phase space ($p_x - x$) (middle) and the electrostatic fields with ion densities distribution along the x axis (bottom) at different times are shown in Fig. 2. From Figs. 2(a) and 2(d) we see that at $t = 52T_L$, the protons are slightly accelerated by TNS at the rear side of the target but do not move forward a lot (also see Figs. 3(a) and 3(d) for comparison). There are clearly two peaks of the electrostatic field located respectively inside the target and at the rear side of the target, corresponding to the shock and TNS in Fig. 2(g). At this moment the protons are affected mainly by the TNSA. At $t = 64T_L$, The shock transmits to the rear side of the target and the electrostatic field of shock almost superposes over that of TNS (see Fig. 2(h)). The protons are accelerated by both the shock and the TNS. At $t = 84T_L$, the laser pulse has left the target and the protons are only accelerated by the TNS (see Fig. 2(i)).

The corresponding ion position (top), ion phase space ($p_x - x$) (middle) and the electrostatic fields with particle densities distribution along the x axis (bottom) at different times in the case of LP pulse are shown in Fig. 3. In the case of LP, the electron heating is more efficient than in the CP case and the TNSA is therefore more efficient. So, the proton layer is accelerated more acutely than in the case of CP at the early time (also see Figs. 2(a) and 2(d) for comparison). However, we find in Fig. 3 that the shock acceleration is less efficient than that in the CP case because of the higher plasma temperature in the LP

case. As a result protons and C^{6+} ions gain less energy from the shock acceleration. As a whole, the co-acceleration of the shock and TNSA is weaker than that of the CP case and the ions (both C^{6+} ions and protons) gain lower energy.

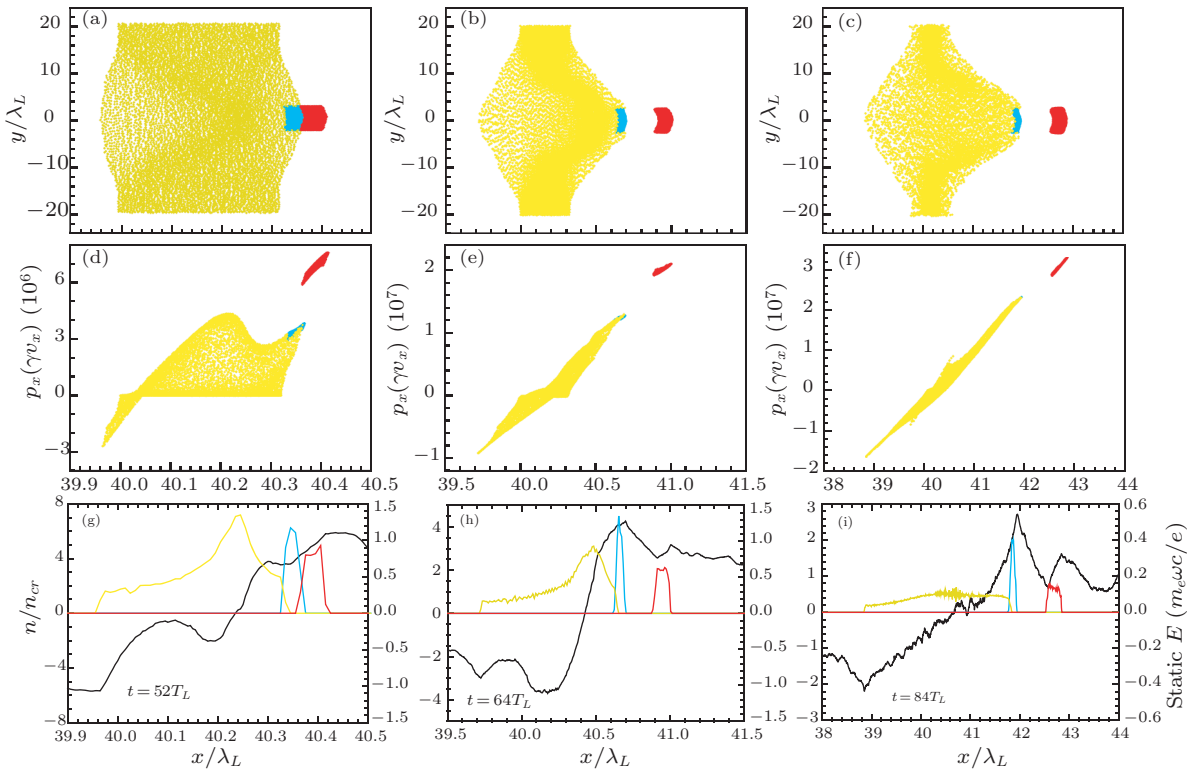


Fig. 3. (Color online) Ion position (top), ion phase space $p_x - x$ (middle) and electrostatic fields with particle densities distribution (bottom) along the x axis at different times under the condition of linearly polarized pulse. All simulation parameters are the same as those in Fig. 2 except the polarization and the dimensionless amplitude $a_L = 5$. The charge number densities of the ions (Zn_c) and the protons (n_p) initially located in the microdot at the rear side of the target have been multiplied by 5 to make them easy to be distinguished.

Figures 4(a) and 4(b) show the electron spatial distribution at $t = 52T_L$ in the CP (left) and LP (right) case. There are both electron sheaths at the rear side of the target in both cases. There are more electrons in the electron sheath in the LP case because the electron heating is more tempestuous. The accelerated electrons in the CP case are produced by the electric field component perpendicular to the plasma surface as we have discussed above. The electron energy spectra are shown in Figs. 4(c) and 4(d). Only the electrons at the rear side of the target are accounted (i.e. the electrons locate after $x = 40.34\lambda_L$). In TNSA, the electrons are accelerated by the laser pulse and propagate through the target to the rear side of the target and form an electron sheath. The electrons in the sheath have a Boltzmann distribution $N = N_0 \exp(-E/k_B T_e)$ which represents a straight line in an energy spectrum plot if the vertical axis is logarithmic coordinate and the electron temperature is proportional to the slope of the line. We can infer from Fig. 4(d) that the electrons in the sheath are almost in Boltzmann's distribution and Fig. 4(c) is similar to Fig. 4(d). Thus, in the CP case the protons which are doped in the rear side of the target can also be accelerated by TNSA, and TNSA also plays an important role in the proton acceleration.

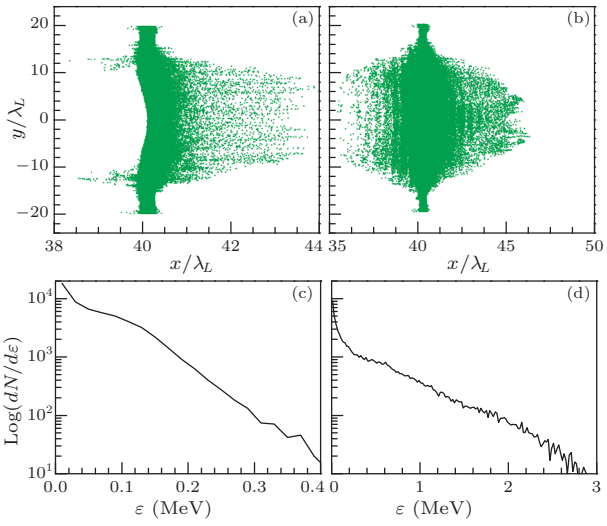


Fig. 4. (Color online) The electron spatial distribution (top) and energy spectra (bottom) at $t = 52T_L$ in the CP (left) and LP (right) case. In (c) and (d), only the electrons at the rear side of the target are accounted.

The transfer efficiency from laser to proton in the LP and CP cases at different times is shown in Fig. 5. The solid and dashed lines represent respectively the CP and LP case. First, the transfer efficiency from laser energy to proton energy in the LP case is much

higher than that in the CP case. However, the transfer efficiency of the CP case rapidly exceeds that of the LP case at about $63T_L$ and finally is about twice as much as that of the LP case, which means that the transfer efficiency from laser to proton in the CP case is higher than that in the LP case. Although the electron heating is more tempestuous and the TNSA is more efficient in the case of LP, the stronger shock acceleration in the case of CP can compensate for the acceleration efficiency.

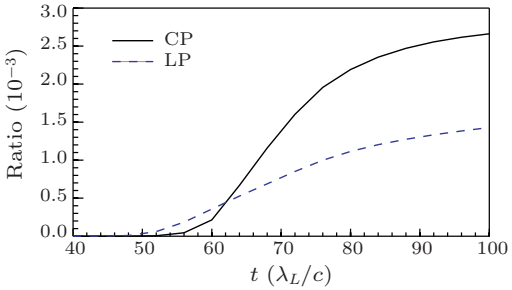


Fig. 5. (Color online) The transfer efficiency from laser to proton in the LP and CP case at different times. The solid and dashed lines represent respectively the CP and LP case.

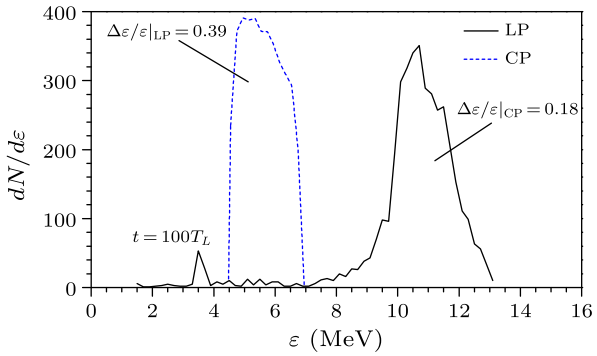


Fig. 6. (Color online) proton energy spectra in the CP (solid line) and LP (dashed line) cases at $t = 100T_L$ when the laser pulse has left the target for $20T_L$.

Figure 6 shows the proton energy spectra in the CP (solid line) and LP (dashed line) cases at $t = 100T_L$ when the laser pulse has left the target for $20T_L$. The energy spread $\Delta\varepsilon/\varepsilon$ (the ratio of the full width at half maximum and the central energy in energy spectra) is also shown in this figure. We find that the central energy of protons in the CP case nearly doubles that in the LP case in Fig. 6, which means that the shock acceleration in the CP case is very important for the proton acceleration in our simulation. The energy spread $\Delta\varepsilon/\varepsilon$ is smaller in the CP case, though the energy spectra in the LP case seems narrow. This is because the central energy of protons in the CP case is higher and the denominator in $\Delta\varepsilon/\varepsilon$ is larger. It should be mentioned that the tail of the proton phase space in Fig. 2(f) corresponds to the peak (solid line in Fig. 6) located at 3.5 MeV. With time, the tail may be left behind the main part of the proton beam. However the tail contains only very small amount of protons, so the energy spread will not be affected heavily by the tail.

In conclusion, we have shown the interaction of a CP laser pulse with a nano-scale micro-structured target with protons which are doped in the rear side of the target by the PIC simulation. The proton layer is accelerated by both the electrostatic fields caused by the CP laser driven shock and TNS at the rear side of the target. Although the electron heating is more tempestuous and the TNSA is more efficient in the LP case, the shock acceleration in the CP case is much more efficient than that in the LP case and can compensate for the comparatively lower efficiency of the TNSA energy compared to the LP case. Consequently, the protons can be accelerated to a higher velocity than that of LP case. With our simulation parameters, a quasimonoenergetic proton bunch is produced with a central energy of about 11 MeV (the double of that in the LP case) and an energy spread of $\Delta\varepsilon/\varepsilon$ about 0.18. If the target parameters (density, thickness, etc.) are optimized, the higher proton energy can be achieved. This is because the shock acceleration is most effective when the target is opaque to the laser pulses.

References

[1] Mackinnon A J et al 2003 *Appl. Phys. Lett.* **82** 3188
[2] Li C K, Seguin F H et al 2006 *Phys. Rev. Lett.* **97** 135003
[3] Ledingham K W D 2002 *AIP Conf. Proc.* **634** 123
[4] Roth M, Cowan T E et al 2001 *Phys. Rev. Lett.* **86** 436
[5] Yang Q S, Liu C et al 2009 *Chin. Phys. Lett.* **26** 065204
[6] Snavely R A, Key M H et al 2000 *Phys. Rev. Lett.* **85** 2945
[7] Hegelich B M, Albright B J et al 2006 *Nature* **439** 441
[8] Schwoerer H, Pfotenhauer1 S et al 2006 *Nature* **439** 445
[9] Borghesi M et al 2006 *Fusion Sci. Technol.* **49** 412
[10] Zhang X M et al 2007 *Phys. Plasmas* **14** 123108
[11] Yin Y, Yu W et al 2008 *Phys. Plasmas* **15** 093106
[12] Chen M, Sheng Z M et al 2007 *Phys. Plasmas* **14** 113106
[13] Ji L L, Shen B F et al 2008 *Phys. Rev. Lett.* **101** 164802
[14] Badziak J et al 2008 *J. Appl. Phys.* **104** 063310
[15] Albright B J, Yin L et al 2007 *Phys. Plasmas* **14** 094502
[16] Shen B F and Xu Z Z 2001 *Phys. Rev.* E **64** 056406
[17] Esirkepov T et al 2004 *Phys. Rev. Lett.* **92** 175003
[18] Robinson A P L et al 2007 *Phys. Rev.* E **75** 015401
[19] d'Humières E et al 2005 *Phys. Plasmas* **12** 062704
[20] He F, Xu H et al 2006 *Phys. Plasmas* **13** 073102
[21] Yan X Q, Lin C et al 2008 *Phys. Rev. Lett.* **100** 135003
[22] Robinson A P L et al 2008 *New J. Phys.* **10** 013021
[23] Liseikina T V et al 2007 *Appl. Phys. Lett.* **91** 171502
[24] Berezhiani1 V I et al 2006 *Europhys. Lett.* **76** 70